IEEE Access
Multidisciplinary ⋮ Rapid Review ⋮ Open Access Journal

Received February 28, 2021, accepted March 12, 2021, date of publication March 17, 2021, date of current version March 23, 2021.

Digital Object Identifier 10.1109/ACCESS.2021.3066415

Joint Range Estimation Using Single Carrier Burst Signals for Networked UAVs

XI PAN[1], CHAOXING YAN[2], (Member, IEEE), AND JIANKANG ZHANG[3], (Senior Member, IEEE)

[1]School of Mechatronical Engineering, Beijing Institute of Technology, Beijing 100081, China
[2]Beijing Research Institute of Telemetry, Beijing 100076, China
[3]Department of Computing and Informatics, Bournemouth University, Poole BH12 5BB, U.K.

Corresponding author: Xi Pan (panxi@bit.edu.cn)

This work was supported in part by the Youth Outstanding Talent Support Program of China Aerospace Science and Technology Corporation, in part by the Key Project of the Key Research Development Program, Ministry of Science and Technology, China, under Grant 2018YFC1407200 and Grant 2019YFC1510904, in part by the National Natural Science Foundation of China under Grant 61571401, and in part by the Innovative Talent of Colleges and University of Henan Province under Grant 18HASTIT021.

ABSTRACT The localization accuracy demand is ever growing in UAV communication networks. We propose a joint coarse and fine range estimation method using single carrier burst signals with two samples per symbol for UAV networks. The coarse estimation of our joint estimation method exploits multiple preamble symbols for flexible single-carrier frequency-domain equalization (SC-FDE) frame structures to calculate correlation metrics, which are insensitive to frequency offset due to the differential correlation operation. Then, we propose a fine range estimation method using only two samples per symbol with expectation relying on shaping or matched filter. Furthermore, we derive the performance bounds for the ranging system using both raised cosine (RC) and better than raised-cosine (BTRC) pulses. Finally, extensive simulations are conducted to validate the proposed method in terms of estimate bias and variance for different modulations, shaping filters, and fading channels. Our simulation results show that, the root mean square errors of proposed ranging method can reach the order of centimeter at medium-to-high signal-to-noise ratio (SNR) region, whereas the case using BTRC filter is capable of enhancing the ranging performance at low SNRs.

INDEX TERMS UAV networks, range estimation, SC-FDE, oversampled signals, two samples per symbol, fading channel, burst signals.

I. INTRODUCTION

Networking node location and pose information can enable group behavior and functionality that would otherwise be impossible [1]. In military scenarios, 3D wireless networks relying on multiple unmanned aerial vehicles (UAVs) can be used for connecting aircraft, troops and fleets, allowing flexible exchange of data between them, and whilst ensuring the security of sensitive information that may be exchanged [2]. Typically, the UAVs will be equipped with a global positioning system (GPS) and an inertial measurement unit (IMU) by regulations in most countries for providing position information at any time, with a positioning accuracy ranging from 6 m to 10 m. When conventional global navigation satellite systems suffer from unacceptable vulnerabilities, such as signal occlusion, spoofing, and jamming, particularly for mission-critical operations, ranging-based localization methods offer an attractive solution to recover node location, like the multi-dimensional scaling (MDS) method [1], [3]. Highly accurate range measurement is also desired mostly for localization purposes in variety of commercial and military applications, such as maintaining a prescribed flight formation in swarming UAVs or munitions, localizing elements of cyber-physical systems for surveillance and exploration [4], [5].

The associate editor coordinating the review of this manuscript and approving it for publication was Wei Feng.

A. UAV COMMUNICATION AND POSITIONING

Usually, common multiple-UAV missions involve at least 3 UAVs [6], [7]. The UAV networking extends the capability of unmanned aircraft system (UAS) and maintains system responsibility and accountability in the face of UAS failure. Bekmezci *et al.* [8] firstly proposed the

This work is licensed under a Creative Commons Attribution 4.0 License. For more information, see https://creativecommons.org/licenses/by/4.0/

multiple-UAV system based on the concept of flying ad hoc network (FANET). Hayat *et al.* [9] overviewed the general networking related requirements, network characteristics and communication requirements of multiple-UAV networks for civil applications. Oubbati *et al.* [10] further presented a survey of position-based routing protocols for FANETs, and classified them into three categories: topology-, swarm-, and position-based routing protocols. The meshed airborne communication architecture offers the best option in terms of flexibility, reliability, and performance compared with other possibilities [11]. Physically smaller UAVs with limited capacity are preferred in FANET applications, like the very low cost close-range UAVs which usually have a flight-span of about 5 km - 15 km [12]. The UAV networking includes four kinds of architectures:

- centralized UAV network architecture having a central ground station node.
- UAV ad hoc network networking a group of similar UAVs.
- multi-group UAV network combining a centralized UAV network and UAV ad hoc networks.
- multi-layer UAV ad hoc network, connecting multiple groups of heterogeneous UAVs and implementing the one-to-many UAV operation mode [13].

The network architectures or UAV formations should be maintained using timely updated position information especially for ''man-in-the-loop'' or intelligent missions [14]. To optimize the communication coverage performance in UAV networks, Khuwaja *et al.* [5] studied the deployments of multiple UAVs as aerial base stations relying on the separation distance between UAVs.

Recently, joint communication and positioning in mobile radio systems has gained a lot of interests in rapid deployment for both civilian and military applications [15]–[17]. Traditionally, one of the most popular ways to obtain location information relied on Radar, where dedicated radio frequencies are allocated to optimize the range and speed estimation performances [18]. While there are many classes of localization techniques, high resolution range estimation is one of key techniques to enable or improve range-based radio positioning, particularly for line of sight (LOS) environment in wireless sensor networks, Internet-of-things (IOT), and machine-to-machine (M2M) communication [19]. UAV communication links can be broadly classified into two aspects namely, air-to-ground (A2G) communications and air-to-air (A2A) communications, where dominated channels are LOS [14], [20]. UAVs can mounted with different-resolution cameras or video cameras [21], ultrasonic, infrared and laser range sensors [22] required for specific missions. These payload data information will be modulated, transmitted and relayed to the UAV ground station (GS) command and control center. In multiple-UAV networks, the UAV position can be determined based on the range estimate from different transmitters, whereas the UAV position can also be calculated using standard techniques [23]–[25]. Range-based localization is possible via the signal time-of-arrival (ToA), time-difference-of-arrival (TDoA), received signal strength (RSS) and direction of arrival (DoA) or their combinations. ToA estimation has received considerable attention among all range based approaches because of high precision and low complexity.

Ultra-wide bandwidth (UWB) signals are commonly used in the localization community having extremely large bandwidth, which can lead to relatively fine time resolution for indoor positioning with short-range coverage [26]. Cyclic prefixed single carrier (CP-SC) and its variations were chosen as the waveforms for joint radar-communication [15], and by a few standards like IEEE 802.11ad and LTE-advanced [27], [28]. Single carrier with frequency domain equalization (SC-FDE) is a popular CP-SC modulation scheme for UAV communication. Principal superiorities of SC-FDE over OFDM are its lower peak-to-average power ratio (PAPR) and less sensitivity to carrier-frequency offset (CFO) while achieving similar equalization performance and ranging accuracy. The data format of an unique-word based single carrier (UW-SC) system [29] is generally composed of data blocks, each preceded with an UW such that low-complexity and accurate frequency-domain channel equalization can be effectively applied. In the SC-FDE receiver architecture of some related works [30], [31], symbol timing synchronization algorithms were usually designed using the cyclic prefix or cyclic suffix sequence with one sample per symbol, following the conventional auto-correlation based timing metric in OFDM system [32]–[34]. The fine ranging method in our previous work [29] relying on the amplitude nonlinearity of oversampled signals in SC-FDE receiver required four samples per symbol to achieve a root mean square error (RMSE) by the order of centimeter at medium-to-high signal-to-noise ratio (SNR) region for a channel bandwidth of 10 MHz. In this paper, we focus on the joint communication and propagation delay-based ranging using single carrier burst signals for networked UAVs.

B. MOTIVATIONS AND CONTRIBUTIONS

The high performance, highly integrated radio frequency (RF) transceiver AD9361 [35] designed for use in 4G base station applications with tunable channel bandwidth is commonly exploited for low-cost solution of UAV communication transceiver. Its data ports can be configured in either single-ended CMOS format with 61.44 MHz data clock or differential low voltage differential signaling (LVDS) format with 122.88 MHz. Considering this dilemma between limited analog-digital conversion (ADC) sampling clock and the requirement of increasing sampling rate, like the ranging method using four samples per symbol in broadband UAV communication [29], we devote efforts to designing enhanced ranging method in SC-FDE receivers using less samples without performance degradation.

Our main contributions in this paper are summarized as follows.

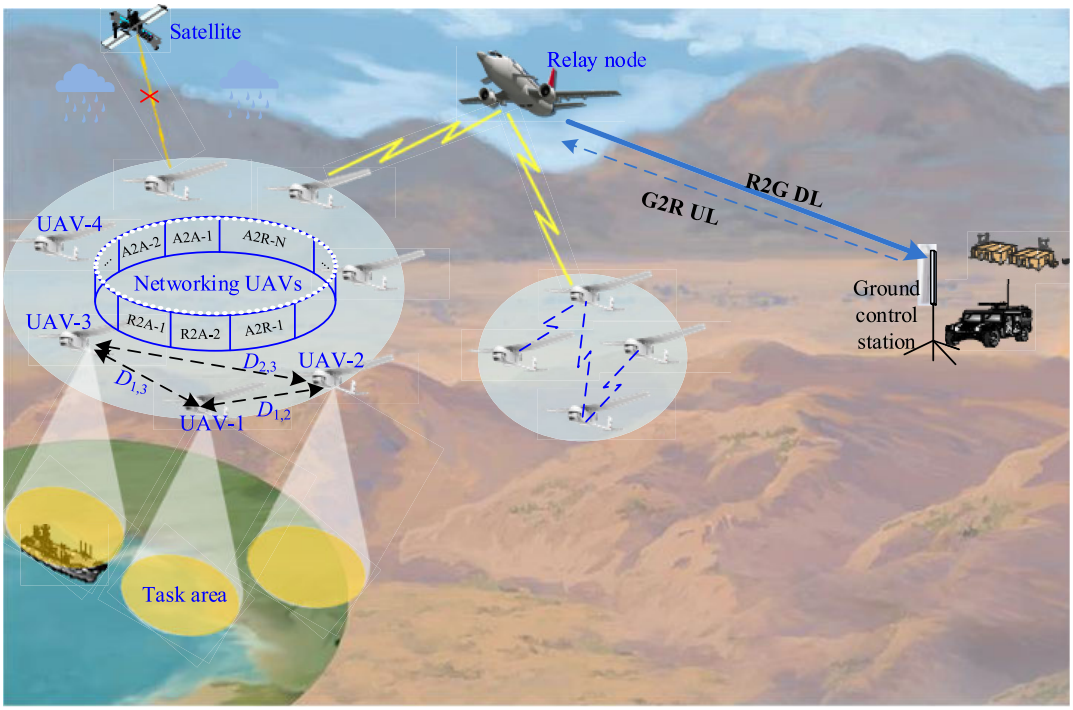

FIGURE 1. UAV networking scenarios with A2G, A2A communication links and ranging among UAVs.

- We propose a joint coarse and fine range estimation method for multiple-UAV networks based on the preamble and payload data in SC-FDE frame respectively, using two samples per symbol for common linear modulations. This method is insensitive to frequency offset and it is capable of enabling UAV communication system to increase signal bandwidth in low-cost digital receivers with limited ADC clock.
- A flexible SC-FDE burst frame is designed for UAV networks containing preamble, UW and payload data segments. Combining the multiple preambles in each slot frame, we calculate correlation metrics using two branches of oversampled preamble sequences to get the preamble position and suggest a multi-dwell strategy to improve position estimation accuracy.
- The proposed fine range estimation method uses only two samples per symbol with expectation relying on shaping or matched filters. The range estimate Cramer-Rao bounds (CRBs) for raised cosine and better than raised-cosine pulses are presented as performance benchmarks in extensive simulations. Our results demonstrate the feasibility and efficiency of the proposed technique in terms of estimate bias and variance for different modulations and shaping filters under both flat-fading channel and frequency selective fading channel.

The rest of this paper is organized as follows. Section II presents the UAV networking scenarios with different communication links and the SC-FDE signal models with flexible burst frame. In Section III, we propose a joint range estimation method and give the coarse ranging method based on the preamble segment. Then, we propose a fine ranging method and analyze the range estimate performance bounds for different shaping filters. Section IV presents the simulation results and discussions, and finally Section V concludes the paper.

II. SYSTEM AND SIGNAL MODELS

A. MULTIPLE-UAV NETWORKING

As depicted in Fig. 1, UAV networking scenarios with A2G communication, A2A communication are composed of ground control station, small task UAVs, and the relatively large UAS working as relay node. Small UASs with highly mobility and limited payload space require lightweight, low-profile, conformal and lower cost omnidirectional antennas, which will absorb multipath signals at receiver due to the broad beamwidth. The channel access strategy for UAV networking is vital in that every node within the UAV swarm should communicate and range at least with its neighbors. Access collisions on the medium access control (MAC) layer lead to undesirably low ranging update rates, particularly for UAVs with high relative mobility. Contention-based MAC schemes suffer from multiple access interference, resulting in unpredictable ranging update rate [36], whereas reservation-based time division multiple access (TDMA) enables interference-free channel access for all users but commonly requires a dedicated master user to establish time slot reservation and scheduling [37].

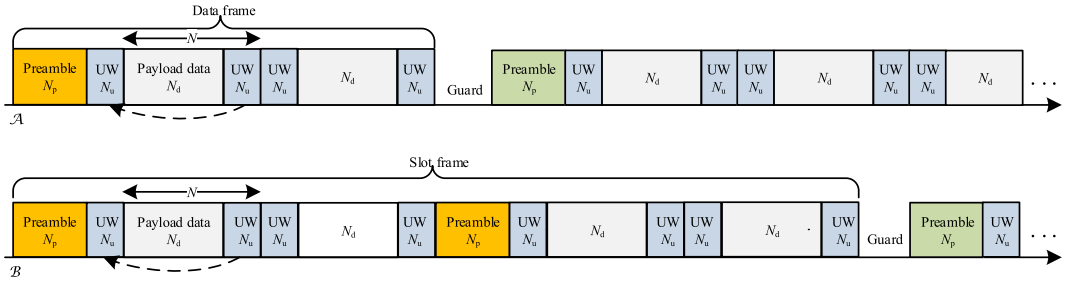

FIGURE 2. Block structures with different SC-FDE burst frames for UAV communications.

There are telemetry datalinks of relay-to-ground (R2G) downlink and ground-to-relay (G2R) uplink, whereas there are also A2A links, air-to-relay (A2R), and relay-to-air (R2A) links among UAVs and relay aircraft. The range between them can be determined by the two-way signals in these communication links, as the $D_{1,2}, D_{1,3}, D_{2,3}$ among UAV-1, UAV-2 and UAV-3 given in Fig. 1. The current popular transmission signals of single carrier and multicarrier are reasonable in different channels and application environments. SC-FDE can mitigate the multipath fading for UAV communications and obtain similar performance, efficiency, and low signal processing complexity advantages compared with OFDM [38]. Moreover, it is insensitive to power amplifier nonlinearities, and it enables the use of a simple power amplifier [39]. Afran *et al.* [40] found that FDE is about 7 times more computationally efficient than the time domain equalizer in the integrated network enhanced telemetry system. SC-FDE techniques have been popularly applied to many modern wireless communication systems with different frame structures, such as IEEE 802.11.ad and IEEE802.16 wireless metropolitan area network (WirelessMAN) standard [41]. In the following text, we will give the burst frame employed in the UAV communication network.

B. SC-FDE BURST FRAME

The SC-FDE data block formats, $\mathcal{A}$ data frame and $\mathcal{B}$ slot frame, are typically presented in Fig. 2, where the data frame is equal to the slot frame for format $\mathcal{A}$. For each data frame, there is one preamble section, preceding by UWs and payload data segments. Define the m-th block of sequence vector as, $\boldsymbol{s}_m$,

$$\boldsymbol{s}_m = [\boldsymbol{s}_{P,N_p}, \boldsymbol{s}_{UW,N_u}, \boldsymbol{s}_{D,N_d}, \boldsymbol{s}_{UW,N_u}], \tag{1}$$

where $\boldsymbol{s}_{P,N_p}$ is the preamble sequence, $\boldsymbol{s}_{UW,N_u}$ is the UW sequence, $\boldsymbol{s}_{D,N_d}$ is the payload data sequence, and N_p, N_u, N_d are length of these sequences, respectively. Since the UW sequence is known in advance at the receiver, the preceding UW sequence can be served as the CP of its following one. The UW also possesses the constant amplitude zero auto-correlation (CAZAC) property [30]. The transmitted signals are represented as,

$$\begin{aligned}\boldsymbol{s}_m = [&s_{m,-N_u-N_p}, \ldots, s_{m,-N_u-1}, s_{m,-N_u}, \ldots, s_{m,-1} \\ &s_{m,0}, s_{m,1}, \ldots, s_{m,N_d-1}, s_{m,N_d}, \ldots, s_{m,N-1}]^T,\end{aligned} \tag{2}$$

where $N = N_u + N_d$ is the FFT length in SC-FDE, $s_{m,n}$ are the complex valued transmitted symbols under different modulation formats such as M-ary phase-shift keying (MPSK) or M-ary quadrature amplitude modulation (MQAM), with mean power 1.

The format $\mathcal{A}$ data frame has N_B blocks of data sequence, which usually are the divided N_B segments of forward error correction codes, like Turbo codes or low-density parity check (LDPC) codes. Thus, the m-th block of sequence in format $\mathcal{A}$ can be described as,

$$\boldsymbol{s}_m = [\boldsymbol{s}_{P,N_p}, \boldsymbol{s}_{UW,N_u}(m), \boldsymbol{s}_{D,N_d}(m), \boldsymbol{s}_{UW,N_u}(m)]. \tag{3}$$

For the data frame with N_B blocks, we rewrite the sequence as,

$$\begin{aligned}\boldsymbol{s}_{m,N_B} = [&\boldsymbol{s}_{P,N_p}, \boldsymbol{s}_{UW,N_u}(1), \boldsymbol{s}_{D,N_d}(1), \boldsymbol{s}_{UW,N_u}(1), \\ &\boldsymbol{s}_{UW,N_u}(2), \boldsymbol{s}_{D,N_d}(2), \boldsymbol{s}_{UW,N_u}(2), \ldots, \\ &\boldsymbol{s}_{UW,N_u}(N_B), \boldsymbol{s}_{D,N_d}(N_B), \boldsymbol{s}_{UW,N_u}(N_B)]^T.\end{aligned} \tag{4}$$

For the UAV node allocated more than one data frame as described by the block format $\mathcal{B}$ in Fig. 2, a slot frame with two data frames can be similarly written as,

$$\begin{aligned}\boldsymbol{s}_{m,2N_B} = [&\boldsymbol{s}_{P,N_p}(1), \boldsymbol{s}_{UW,N_u}(1), \boldsymbol{s}_{D,N_d}(1), \boldsymbol{s}_{UW,N_u}(1), \\ &\boldsymbol{s}_{UW,N_u}(2), \boldsymbol{s}_{D,N_d}(2), \boldsymbol{s}_{UW,N_u}(2), \ldots, \boldsymbol{s}_{UW,N_u}(N_B), \\ &\boldsymbol{s}_{D,N_d}(N_B), \boldsymbol{s}_{UW,N_u}(N_B), \boldsymbol{s}_{P,N_p}(2), \boldsymbol{s}_{UW,N_u}(N_B+1), \\ &\boldsymbol{s}_{D,N_d}(N_B+1), \boldsymbol{s}_{UW,N_u}(N_B+1), \boldsymbol{s}_{UW,N_u}(N_B+2), \\ &\boldsymbol{s}_{D,N_d}(N_B+2), \boldsymbol{s}_{UW,N_u}(N_B+2), \\ &\ldots, \boldsymbol{s}_{UW,N_u}(2N_B), \boldsymbol{s}_{D,N_d}(2N_B), \boldsymbol{s}_{UW,N_u}(2N_B),]^T,\end{aligned} \tag{5}$$

where two data frames comprise the slot frame, and we can also generalize this expression with more data frames. We suggest to make full use of the multiple data frames in one slot frame to improve the ranging performance, whereas there is a tradeoff between enhanced ranging accuracy and increased delay for mission-critical operations.

III. JOINT RANGE ESTIMATION WITH TWO SAMPLES PER SYMBOL

A. PROPOSED JOINT RANGE ESTIMATION METHOD

Compared with OFDM techniques, the synchronization and estimation for SC-FDE system is much less examined in the literature. Following the method designed for OFDM [32], the conjugate product between two successively received UW

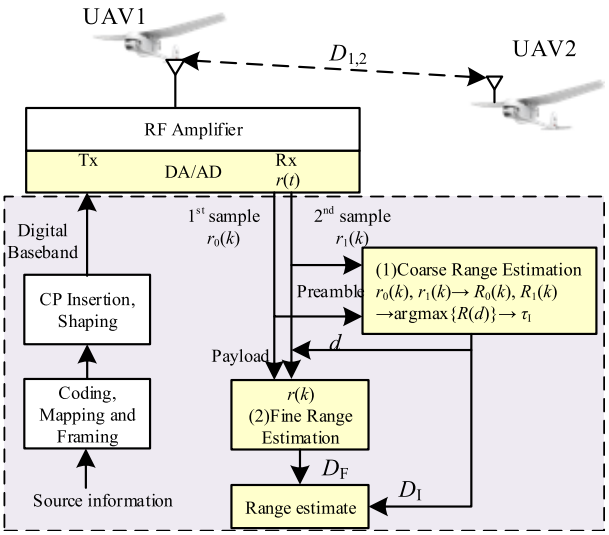

FIGURE 3. Block structure for range estimation between networked UAVs, with two samples per symbol in SC-FDE receiver.

blocks in SC-FDE receiver will exhibit the timing metric plateau resulting in a degraded variance of the timing estimate at low SNRs [42]. Chiang *et al.* [41] estimated the total phase shift due to carrier frequency offset and symbol timing offset using time-domain UW sequences in the frequency domain of SC-FDE. Lin and Chen [43] proposed a blind fine synchronization scheme using the simple weighted least-square method without additional UW sequences.

We present the following joint coarse and fine range estimation method as given in Fig. 3. The source information from UAV1 after coding, mapping and framing will be modulated using SC-FDE scheme by inserting UWs. Then, the transmitted symbols $s(n)$ are filtered with shaping filter and finally converted to analog signals and sent out by radio frequency (RF) power amplifier. After propagation in space between UAV1 and UAV2, the received equivalent complex baseband signal is written as $r(t)$.

$$r(t) = \int h(\varepsilon)x(t-\varepsilon-\tau T)e^{j\phi}d\varepsilon + w(t) \tag{6}$$

where $h(t)$ is the fading channel impulse response, $w(t)$ is the additive white and Gaussian noise (AWGN) with power N_0, τT is the delay, ϕ is the carrier offset, and $x(t)$ is the transmitted complex signals,

$$x(t) = \sum_{n=-\infty}^{\infty} s(n)g_s(t-nT), \tag{7}$$

where $s(n)$ is the transmitted symbol, $g_s(t)$ is the shaping or matched filters.

Assuming the flat-fading channel with unit magnitude, we propose the range estimation procedures at the UAV1 receiver as follows,

1) The received $r(t)$ is oversampled with $T_s = T/2$,

$$r(kT_s) = \sum_{n=-\infty}^{\infty} s(n)g(kT_s - nT - \tau T) + w(kT_s), \tag{8}$$

where $g(t)$ is the convolution of shaping and matched filters, and for the case of raised cosine (RC) filter,

$$g_{RC}(t) = \text{sinc}(\pi t/T)\frac{\cos(\pi t/T)}{1-4\alpha^2t^2/T^2}, \tag{9}$$

where α is the rolling-off factor. Then, we have the two sampling sequences $r_u(k) = r_0(k), r_1(k)$, and $r(k) = \{r_0(k), r_1(k)\}$,

$$\begin{aligned} r_0(k) &= r(2nT_s), \\ r_1(k) &= r(2(n+1)T_s). \end{aligned} \tag{10}$$

2) The correlation metrics $R_u(d) = R_0(d), R_1(d)$ are calculated for two sampling sequences $r_u(k) = r_0(k), r_1(k)$, respectively, as following,

$$\begin{aligned} &R_u(d) \\ &= \frac{\left|\sum_{k=1}^{N_p-1} r_u^*(k+d-1)r_u(k+d)s_p(d-1)s_p^*(d)\right|^2}{\left(\sum_{k=1}^{N_p}|r_u(k+d)|^2\right)^2} \end{aligned} \tag{11}$$

where $s_p(d)$ is the local preamble sequence, and d is the position of preamble sequence in the received slot frame. The denominator term herein normalizes this differential correlation in numerator term by the received total signal power of length N_p.

3) The timing metrics $R_0(d), R_1(d)$ are compared with predefined timing metric threshold λ, as $R_u(d) \geq \lambda$ to find the position d of preamble sequence in the received slot frame, $\hat{d} = \arg\max R(d)$, where $R(d) = \{R_0(k), R_1(k)\}$. Thus, we can arrive at the integer-valued time delay estimation $\tau_I = \hat{d}T_s$.

4) Compute the range between UAV1 and UAV2 as $D = C(\hat{\tau}_I + \hat{\tau}_F) = \hat{D}_I + \hat{D}_F$, where C is the speed of light and $\hat{\tau}_F$ is the fine estimate. We would provide the fine estimation method using the payload data sequence $\boldsymbol{s}_{D,N_d}$ received in $r_u(k)$ in next section.

We note that the timing offset and carrier offset estimations are not required prior to the proposed ranging method. The differential correlation in (11) makes the correlation metrics $R_u(d)$ resistant to carrier offset, and it was also exploited for carrier offset estimation in [44]. Following the proposed coarse ranging method, we examine the correlation metrics as given in Fig. 4, where the simulation for slot frame block format $\mathcal{B}$ is assumed to have two data frames with $N_B = 1$ block of data sequence, $N_p = 64$, $N_d = 960$, $N_u = 64$, and $N = 1024$. The peak timing metric at $k = 64$ and 1280 for two preamble sequences validate the interval between them, $N_p + N_d + 2N_u = 1280 - 64$. We can also find that, $R_0(d)$ for the first sample sequence is much larger

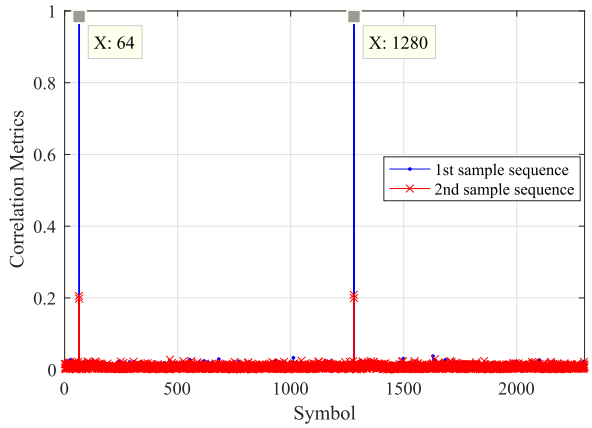

FIGURE 4. Correlation metrics for the ranging method using two samples per symbol with $N_p = 64$, $N_d = 960$, $N_u = 64$, $N_B = 1$ for block format $\mathcal{B}$.

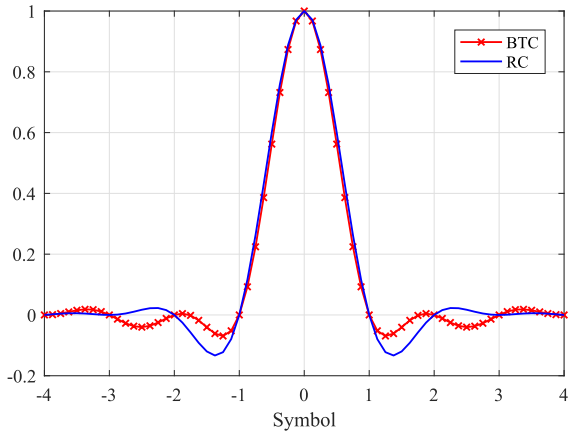

FIGURE 5. Filter coefficients of $g(t)$ for RC and BTRC, $\alpha = 0.5$.

than $R_1(d)$ for the second one at the position d of preamble sequence. For the case with multiple preamble sequences and related metric peaks, we suggest enhancing the accuracy of position d estimation using the multi-dwell strategy [45], which will reduce the false alarm probability P_f and miss detection probability P_m for detecting the position d.

B. FINE RANGE ESTIMATION WITH TWO SAMPLES PER SYMBOL

In this section, we propose a fine range estimation method using two samples per symbol in SC-FDE. The range estimate is given as (12), shown at the bottom of the page, where $\Re$ denotes real part, L is the length of transmitted MPSK or MQAM payload data symbols exploited in the ranging module.

The first two summation terms in (12) involves $2L$ samples, $r(1)$ to $r(2L)$, whereas the third one involves $2L+1$ samples, $r(0)$ to $r(2L-1)$. For any n in (12), it holds that the expectation (13), shown at the bottom of the page, relies on the filter $g(t)$. Similarly, for any n in the third term, it holds that the expectation (14), shown at the bottom of the page, also relies on filter $g(t)$.

These expectations will determine the statistical variance of the proposed range estimation method, whereas this motivates us to exploit the better than raised cosine (BTRC) filter $g(t)$ [46] for the proposed ranging method,

$$g_B(t) = \mathrm{sinc}(\pi t/T)\frac{4\beta t\sin(\pi\alpha t/T)+2\beta^2\cos(\pi\alpha t/T)-\beta^2}{4\alpha^2 t^2/T^2+\beta^2}, \tag{15}$$

where $\beta = (2T\ln 2)/\alpha$. BTRC has smaller maximum distortion compared with RC for the same rolling-off factor α. We will also examine the influence for distinct shaping filters on ranging performance by extensive simulations.

C. ESTIMATION PERFORMANCE BOUND

We use CRB to compare analytically the performance of proposed fine range estimation method, in terms of estimate variance. Following the similar derivations in Chapter 2.4 of [47], the CRB states the variance of range estimates and it is

$$\hat{D}_F = \frac{CT}{2\pi}\arg\left\{\sum_{n=1}^{L}\left\{|r(2n)|^2-|r(2n-1)|^2+j\Re[r(2n)r^*(2n-1)-r(2n-1)r^*(2(n-1))]\right\}\right\}, \tag{12}$$

$$\begin{aligned}&E\left\{r(2nT_s)r^*((2n-1)T_s)-r((2n-1)T_S)r^*(2(n-1)T_s)\right\}\\&=E\left\{x(2nT_s-\tau T)x^*((2n-1)T_s-\tau T)-x((2n-1)T_S-\tau T)x^*(2(n-1)T_s-\tau T)\right\}\\&=\sum_{n=-\infty}^{\infty}\left\{g(\tau T+nT)g(\tau T+(n-0.5)T)-g(\tau T+nT)g(\tau T+(n+0.5)T)\right\}.\end{aligned} \tag{13}$$

$$\begin{aligned}&E\left\{|r(2nT_s)|^2-|r((2n-1)T_s)|^2\right\}\\&=E\left\{|x(2nT_s-\tau T)|^2-|x((2n-1)T_s-\tau T)|^2\right\}\\&=\sum_{n=-\infty}^{\infty}\left\{g^2(\tau T+nT)-g^2(\tau T+(n-0.5)T)\right\}.\end{aligned} \tag{14}$$

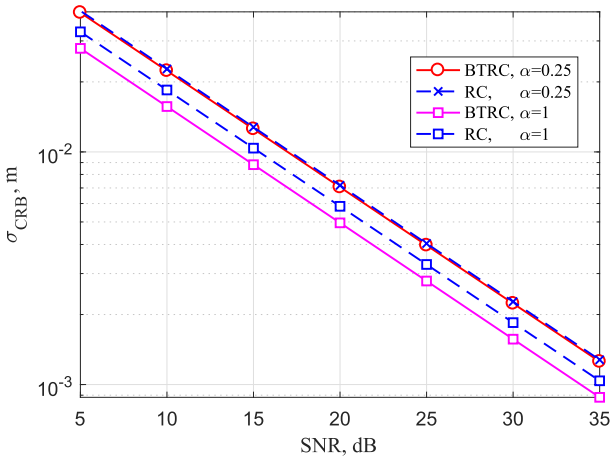

FIGURE 6. Root mean square value for CRB of range estimate with RC and BTRC filters, $L = 1024$.

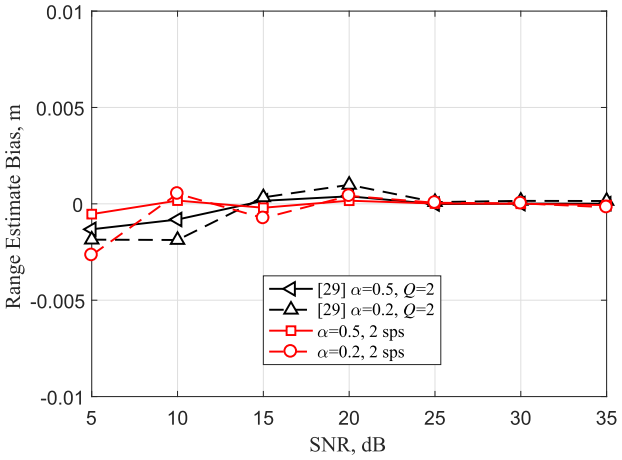

FIGURE 7. Bias of the proposed range estimation method and the method in [29] with QPSK signals at different SNRs, $\alpha = 0.2$ and 0.5.

lower bounded as,

$$\mathrm{Var}[\hat{D}_F - D_F] \geq \frac{C^2}{2LE_s/N_0} \times \frac{\int_{-\infty}^{\infty} G(f)df}{\int_{-\infty}^{\infty} 4\pi^2 f^2 G(f)df} \doteq CRB, \tag{16}$$

where $G(f)$ is the Fourier transform of the filter $g(t)$, E_s is the signal power and N_0 is the noise power. When raised cosine filter is used, the CRB of range estimate is given as,

$$CRB_{RC} = \frac{3C^2T^2}{2LE_s/N_0} \times \frac{1}{3(\pi^2-8)\alpha^2+\pi^2}. \tag{17}$$

The CRB for better than raised-cosine pulses can be derived as,

$$CRB_{BTRC} = \frac{3C^2T^2}{2\pi^2 LE_s/N_0} \times \frac{1}{1+6(1-2\ln 2+(\ln 2)^2\alpha^2)\alpha^2/(\ln 2)^2}. \tag{18}$$

In order to evaluate estimation performance, RMSE is adopted as the comparison measure with CRB as a benchmark. The RMSEs corresponding to CRBs for raised cosine filter and better than raised-cosine, $\sigma_{D,CRB} = \sqrt{CRB_{RC}}$ or $\sqrt{CRB_{BTRC}}$, are depicted in Fig. 6 as "RC" and "BTRC" under different $\alpha = 0.25$ and 1. We find that, for the smaller α, the gap between CRB_{RC} and CRB_{BTRC} will get narrower.

IV. RESULTS AND DISCUSSIONS

In the following section, we investigate the performance of proposed ranging method for SC-FDE system in terms of estimation bias and RMSE performance under different parameters. The previous work [29] is compared as a performance reference, where the fine ranging method is,

$$\hat{D}_F = \frac{CT}{2\pi} \arg\left\{\sum_{k=0}^{4L-1} |r(kT_s)|^Q e^{-j2\pi k/4}\right\}, \tag{19}$$

where $Q = 2$ is the designed parameter when oversampling factor is $T_s/T = 4$.

An SC-FDE system with BPSK, QPSK, 8PSK and 16PSK modulations, rolling off factors $\alpha = 0.2, 0.25, 0.35, 0.5$, data block length of $N = 1024$, UW length of $N_u = 64$, bandwidth of 50 MHz and normalized carrier frequency offset of 5×10^{-3}, has been considered with extensive simulations in flat-fading channel and frequency-selective fading channel to validate our proposed ranging method. CRBs for raised cosine and better than raised-cosine pulses are also compared as performance benchmarks. The parameters are summarized in Table 1.

TABLE 1. Parameters setting in simulations.

Parameter	Values
Modulation	BPSK, QPSK, 8PSK, 16PSK
Rolling off factor α	0.2, 0.25, 0.35, 0.5
Block length L	1024
Preamble length	64
UW length	64
Bandwidth	50 MHz
Channel	Rician, AWGN
Rice factor, K	10 dB

A. RANGE ESTIMATE BIAS

Figure 7 presents the estimation bias performance of the proposed ranging method (12) and the method (19) in [29], denoted as "2 sps (samples per symbol)" and "4 sps", respectively, under different rolling off factors $\alpha = 0.2, 0.5$. We can find that, the bias values of both methods get close to zeros under high SNR $\geq$ 25 dB, whereas there are fluctuations on the order of 0.002 m under low SNR. The range estimate bias performance holds the same characteristics for BPSK, QPSK, 8PSK and 16PSK with $\alpha = 0.5$ as depicted in Fig. 8. The range estimate is not sensitive to carrier frequency offsets arising from UAV high mobility due to the differential correlations employed. These estimate bias fluctuation above results from channel noises and limited simulations. Therefore, for different modulations adopted in payload data segment in Fig. 2, we can always employ the proposed ranging method in UAV networks.

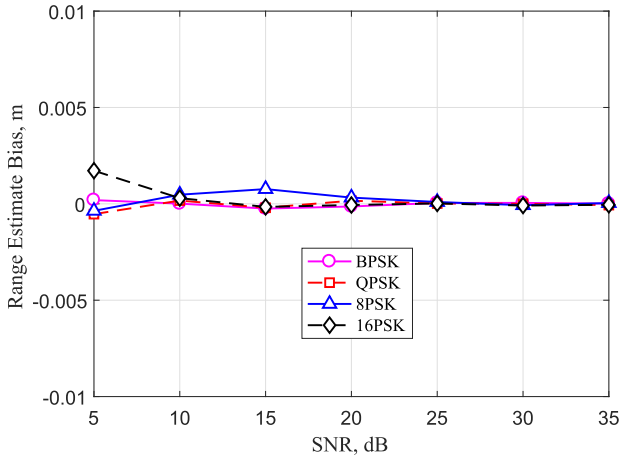

FIGURE 8. Bias of the proposed range estimation method (12) for SC-FDE system with BPSK, QPSK, 8PSK and 16PSK signals at different SNRs, $\alpha = 0.5$.

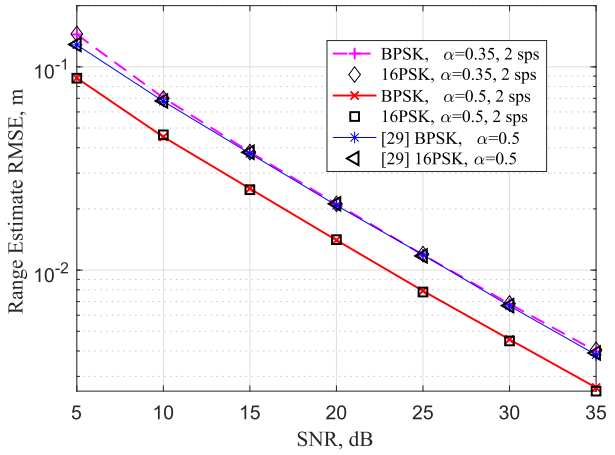

FIGURE 10. RMSE of the proposed range estimation method (12) and the method in [29] with BPSK and 16PSK signals at different SNRs, α =0.35 and 0.5.

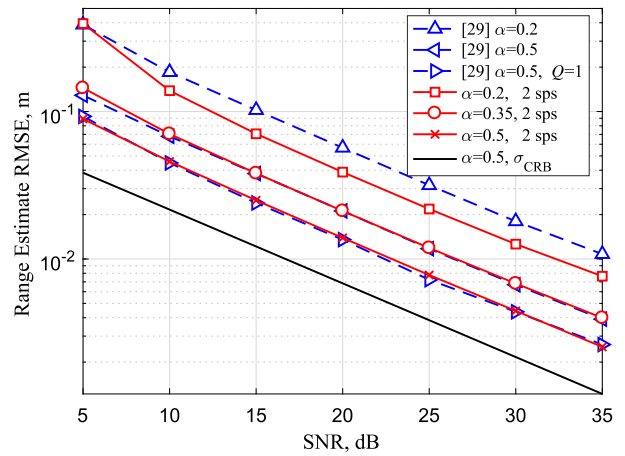

FIGURE 9. RMSE of the proposed range estimation method (12) and the method in [29] with QPSK signals at different SNRs, α =0.2, 0.35 and 0.5.

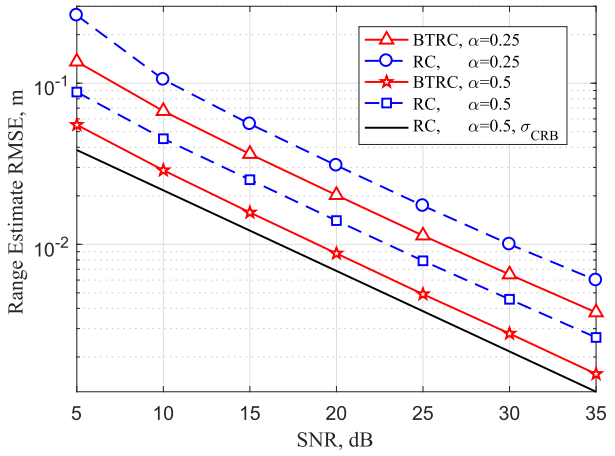

FIGURE 11. RMSE of the proposed range estimation method (12) with QPSK signals using RC or BTRC filters at different SNRs, $\alpha = 0.25$ and 0.5.

B. RANGE ESTIMATE RMSE

Figure 9 depicts the RMSE performance of the proposed ranging method "2 sps" (12) and the previous one (19) for different α. It can be found that, the RMSE of both methods will get close to CRB upon increasing α. For $\alpha = 0.2$, 0.35, 0.5, the method "2 sps" reaches 0.138 m, 0.07 m, 0.045 m respectively, at SNR = 10 dB. However, the proposed ranging method will perform similar to the method using $Q = 1$ in [29] while 3 dB better than $Q = 2$ under the same $\alpha = 0.5$. It gets close to CRB with ranging jitter reaching below 1 cm when SNR $\geq$ 26 dB, 23 dB for $\alpha = 0.35$, 0.5, respectively. The traditional "4 sps" method in [29] with $Q = 2$ was recommended for implementation due to its relative low computation complexity. It is then compared with the proposed ranging method (12) for BPSK and 16PSK, $\alpha = 0.35$, 0.5 in Fig. 10, where the RMSE hold the same characteristics for different modulation schemes. Next, range estimation performance of the proposed "2 sps" method versus SNR as well as $\alpha = 0.25$, 0.5 using both RC and BTRC filters are provided in Fig. 11. Results show that the enhancements by the BTRC filter are more obvious than RC filter at low SNRs. For $\alpha = 0.25$, 0.5, the method "BTRC" reaches 0.067 m, 0.028 m respectively, at SNR = 10 dB.

Finally, we examine the RMSE performance of the proposed ranging method in frequency-selective channel for QPSK signals using RC and BTRC filters, with $\alpha = 0.5$, as illustrated in Fig. 12. The Rician fading channel is modelled as 5 paths with path delays of $k = 1$, 3, 5, 7, 9 samples exponentially decaying path gains of $e^{-\varepsilon_k/3}$ and K factor of 10 dB [12], [48]. Performance degradation exists in this frequency-selective channel with a floor of about 0.1 m for both filters, whereas channel estimation and frequency-domain equalization will improve the RMSE performance [49]. The proposed ranging method in frequency-selective channel will achieve performance close to that in flat-fading channel if it is preceded by perfect channel state information and channel equalization for oversampled signals in SC-FDE receivers. For both cases of the ranging methods with and without channel equalizations, the method using BTRC filter will outperform the RC one at low SNR regions, by about 0.02 m at SNR = 5 dB.

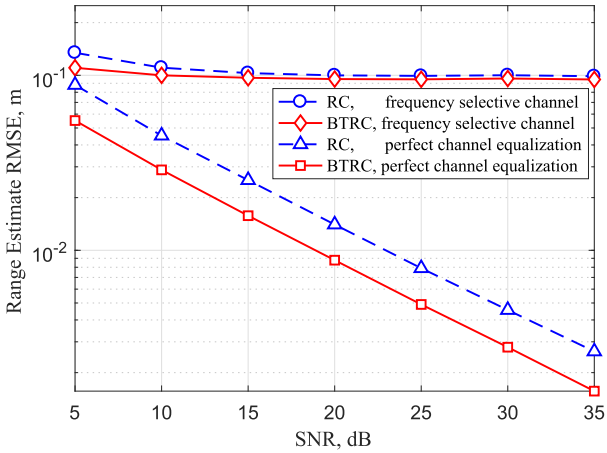

FIGURE 12. RMSE of the proposed range estimation method (12) under fading channels with RC and BTRC, QPSK signals, $\alpha = 0.5$.

C. COMPUTATIONAL COMPLEXITY

The computational complexity is further analyzed following the way in [50]. The traditional ranging method in [29] requires $8L + 1$ real multiplications, $2(L - 1)$ additions and 1 phase arg operation, whereas the proposed fine ranging method (12) requires $6L+1$ real multiplications, $4L$ additions and 1 phase arg operation. The multiplication resources are more critical than additions for most implementation scheme like Field Programmable Gate Array (FPGA). Therefore, the proposed method could achieve accurate range estimate at low cost of computation complexity, while it requires lower sampling rate than previous methods. The low sampling rate requirement will make the transceiver AD9361 applicable in broadband communication and ranging for low-cost UAV swarms.

V. CONCLUSION

The localization accuracy of navigation and radar systems in UAV networks is affected by the quality of range information. Joint radar-communication would bring more efficient plan and usage for the radio spectral resource. We propose a ranging method constitutes of coarse ranging and fine ranging procedures for joint communication and positioning applications. After presenting the UAV networking scenarios with different communication links and the SC-FDE signal models with flexible burst frame, we propose the coarse ranging method based on the preamble segment. Then, we propose the fine ranging method and analyze the performance bounds for different shaping filters. Extensive simulations illustrate that the proposed method can reach the order of centimeter in terms of range estimate RMSE at medium-to-high SNR region under different conditions and this method is insensitive to carrier frequency offset. We also suggest using BTRC filter to enhance the performance at low SNRs.

REFERENCES

[1] M. Hamaoui, "Non-iterative MDS method for collaborative network localization with sparse range and pointing measurements," *IEEE Trans. Signal Process.*, vol. 67, no. 3, pp. 568–578, Feb. 2019.

[2] X. Li, W. Feng, Y. Chen, C.-X. Wang, and N. Ge, "Maritime coverage enhancement using UAVs coordinated with hybrid satellite-terrestrial networks," *IEEE Trans. Commun.*, vol. 68, no. 4, pp. 2355–2369, Apr. 2020.

[3] W. Yuan, N. Wu, B. Etzlinger, Y. Li, C. Yan, and L. Hanzo, "Expectation–maximization-based passive localization relying on asynchronous receivers: Centralized versus distributed implementations," *IEEE Trans. Commun.*, vol. 67, no. 1, pp. 668–681, Jan. 2019.

[4] E. Staudinger, S. Zhang, and A. Dammann, "Cramér-Rao lower-bound for round-trip delay ranging with subcarrier-interleaved OFDMA," *IEEE Trans. Aerosp. Electron. Syst.*, vol. 52, no. 6, pp. 2961–2972, Dec. 2017.

[5] A. A. Khuwaja, G. Zheng, Y. Chen, and W. Feng, "Optimum deployment of multiple UAVs for coverage area maximization in the presence of co-channel interference," *IEEE Access*, vol. 7, pp. 85203–85212, 2019.

[6] J.-A. Maxa, M.-S. B. Mahmoud, and N. Larrieu, "Survey on UAANET routing protocols and network security challenges," *Ad Hoc Sensor Wireless Netw.*, vol. 37, nos. 1–4, pp. 231–320, 2017.

[7] K. Namuduri, S. Chaumette, J. H. Kim, and J. P. Sterbenz, *UAV Networks and Communications*. Cambridge, U.K.: Cambridge Univ. Press, 2018.

[8] İ. Bekmezci, O. K. Sahingoz, and Ş. Temel, "Flying ad-hoc networks (FANETs): A survey," *Ad Hoc Netw.*, vol. 11, no. 3, pp. 1254–1270, May 2013.

[9] S. Hayat, E. Yanmaz, and R. Muzaffar, "Survey on unmanned aerial vehicle networks for civil applications: A communications viewpoint," *IEEE Commun. Surveys Tuts.*, vol. 18, no. 4, pp. 2624–2661, Apr. 2016.

[10] O. S. Oubbati, A. Lakas, F. Zhou, M. Güneş, and M. B. Yagoubi, "A survey on position-based routing protocols for flying ad hoc networks (FANETs)," *Veh. Commun.*, vol. 10, pp. 29–56, Oct. 2017.

[11] E. W. Frew and T. X. Brown, "Airborne communication networks for small unmanned aircraft systems," *Proc. IEEE*, vol. 96, no. 12, pp. 2008–2027, Dec. 2008.

[12] C. Yan, L. Fu, J. Zhang, and J. Wang, "A comprehensive survey on UAV communication channel modeling," *IEEE Access*, vol. 7, pp. 107770–107793, 2019.

[13] J. Li, Y. Zhou, and L. Lamont, "Communication architectures and protocols for networking unmanned aerial vehicles," in *Proc. IEEE Globecom Workshops (GC Wkshps)*, Dec. 2013, pp. 1415–1420.

[14] J. Zhang, T. Chen, S. Zhong, J. Wang, W. Zhang, X. Zuo, R. G. Maunder, and L. Hanzo, "Aeronautical *Ad Hoc* networking for the Internet-above-the-clouds," *Proc. IEEE*, vol. 107, no. 5, pp. 868–911, May 2019.

[15] Y. Zeng, Y. Ma, and S. Sun, "Joint radar-communication with cyclic prefixed single carrier waveforms," *IEEE Trans. Veh. Technol.*, vol. 69, no. 4, pp. 4069–4079, Apr. 2020.

[16] X. Pan, C. Yan, and J. Zhang, "Nonlinearity-based single-channel monopulse tracking method for OFDM-aided UAV A2G communications," *IEEE Access*, vol. 7, pp. 148485–148494, 2019.

[17] F. Liu and C. Masouros, "A tutorial on joint radar and communication transmission for vehicular networks—Part I: Background and fundamentals," *IEEE Commun. Lett.*, vol. 25, no. 2, pp. 322–326, Feb. 2021.

[18] X. Pan, C. Xiang, S. Liu, and S. Yan, "Low-complexity time-domain ranging algorithm with FMCW sensors," *Sensors*, vol. 19, no. 14, p. 3176, Jul. 2019.

[19] W. Feng, J. Wang, Y. Chen, X. Wang, N. Ge, and J. Lu, "UAV-aided MIMO communications for 5G Internet of Things," *IEEE Internet Things J.*, vol. 6, no. 2, pp. 1731–1740, Apr. 2019.

[20] A. A. Khuwaja, Y. Chen, N. Zhao, M.-S. Alouini, and P. Dobbins, "A survey of channel modeling for UAV communications," *IEEE Commun. Surveys Tuts.*, vol. 20, no. 4, pp. 2804–2821, Jul. 2018.

[21] S. Minaeian, J. Liu, and Y.-J. Son, "Effective and efficient detection of moving targets from a UAV's camera," *IEEE Trans. Intell. Transp. Syst.*, vol. 19, no. 2, pp. 497–506, Feb. 2018.

[22] N. Gageik, P. Benz, and S. Montenegro, "Obstacle detection and collision avoidance for a UAV with complementary low-cost sensors," *IEEE Access*, vol. 3, pp. 599–609, 2015.

[23] S. Dwivedi, D. Zachariah, A. De Angelis, and P. Handel, "Cooperative decentralized localization using scheduled wireless transmissions," *IEEE Commun. Lett.*, vol. 17, no. 6, pp. 1240–1243, Jun. 2013.

[24] H. Wymeersch, J. Lien, and M. Z. Win, "Cooperative localization in wireless networks," *Proc. IEEE*, vol. 97, no. 2, pp. 427–450, Feb. 2009.

[25] S. Dwivedi, A. De Angelis, D. Zachariah, and P. Händel, "Joint ranging and clock parameter estimation by wireless round trip time measurements," *IEEE J. Sel. Areas Commun.*, vol. 33, no. 11, pp. 2379–2390, Nov. 2015.

[26] S. Wang, G. Mao, and J. A. Zhang, "Joint time-of-arrival estimation for coherent UWB ranging in multipath environment with multi-user interference," *IEEE Trans. Signal Process.*, vol. 67, no. 14, pp. 3743–3755, Jul. 2019.
[27] *IEEE Standard for Local and Metropolitan Area Networks: Enhancements for Very High Throughput in the 60 GHz Band*, IEEE Standard 802.11ac, 2012.
[28] *V14.2.0 Physical Layer Procedures (Release 14)*, document ETSI, 3GPP TS 36.213, 2017.
[29] X. Pan, S. Liu, and S. Yan, "Nonlinearity-based ranging technique in SC-FDE communication system with oversampled signals," *IEEE Access*, vol. 7, pp. 49632–49640, 2019.
[30] J. Blumenstein and M. Bobula, "Coarse time synchronization utilizing symmetric properties of Zadoff–Chu sequences," *IEEE Commun. Lett.*, vol. 22, no. 5, pp. 1006–1009, May 2018.
[31] Y. Yao, X. Dong, and N. Tin, "Design and analysis of timing synchronization in block transmission UWB systems," *IEEE Trans. Commun.*, vol. 59, no. 6, pp. 1686–1696, Jun. 2011.
[32] T. M. Schmidl and D. C. Cox, "Robust frequency and timing synchronization for OFDM," *IEEE Trans. Commun.*, vol. 45, no. 12, pp. 1613–1621, Dec. 1997.
[33] H. Minn, V. K. Bhargava, and K. B. Letaief, "A robust timing and frequency synchronization for OFDM systems," *IEEE Trans. Wireless Commun.*, vol. 24, no. 5, pp. 822–839, May 2003.
[34] G. Ren, Y. Chang, H. Zhang, and H. Zhang, "Synchronization method based on a new constant envelop preamble for OFDM systems," *IEEE Trans. Broadcast.*, vol. 51, no. 1, pp. 139–143, Mar. 2005.
[35] Analog Devices. *RF Agile Transceiver AD9361*. Accessed: 2016. [Online]. Available: https://www.analog.com/media/en/technical-documentation/data-sheets/AD9361.pdf
[36] M. Hadded, P. Muhlethaler, A. Laouiti, R. Zagrouba, and L. A. Saidane, "TDMA-based MAC protocols for vehicular ad hoc networks: A survey, qualitative analysis, and open research issues," *IEEE Commun. Surveys Tuts.*, vol. 17, no. 4, pp. 2461–2492, Jun. 2015.
[37] D. Dardari, A. Conti, U. Ferner, A. Giorgetti, and M. Z. Win, "Ranging with ultrawide bandwidth signals in multipath environments," *Proc. IEEE*, vol. 97, no. 2, pp. 404–426, Feb. 2009.
[38] H. Sari, G. Karam, and I. Jeanclaude, "Transmission techniques for digital terrestrial TV broadcasting," *IEEE Commun. Mag.*, vol. 33, no. 2, pp. 100–109, Feb. 1995.
[39] D. Falconer, S. L. Ariyavisitakul, A. Benyamin-Seeyar, and B. Eidson, "Frequency domain equalization for single-carrier broadband wireless systems," *IEEE Commun. Mag.*, vol. 40, no. 4, pp. 58–66, Apr. 2002.
[40] M. Afran, M. Saquib, and M. Rice, "Frequency domain equalizer for aeronautical telemetry," in *Proc. Int. Telemetering Conf.*, 2015, pp. 1–12.
[41] P.-H. Chiang, D.-B. Lin, H.-J. Li, and G. Stuber, "Joint estimation of carrier-frequency and sampling-frequency offsets for SC-FDE systems on multipath fading channels," *IEEE Trans. Commun.*, vol. 56, no. 8, pp. 1231–1235, Aug. 2008.
[42] S. Reinhardt and R. Weigel, "Pilot aided timing synchronization for SC-FDE and OFDM: A comparison," in *Proc. IEEE Int. Symp. Commun. Inf. Technol. (ISCIT)*, Oct. 2004, pp. 628–633.
[43] Y.-T. Lin and S.-G. Chen, "A blind fine synchronization scheme for SC-FDE systems," *IEEE Trans. Commun.*, vol. 62, no. 1, pp. 293–301, Jan. 2014.
[44] P. Singh, E. Sharma, K. Vasudevan, and R. Budhiraja, "CFO and channel estimation for frequency selective MIMO-FBMC/OQAM systems," *IEEE Wireless Commun. Lett.*, vol. 7, no. 5, pp. 844–847, Oct. 2018.
[45] D. Yang, C. Yan, H. Wang, J. Kuang, H. Zhang, and N. Wu, "Performance evaluation of different detectors for frame synchronization in DVB-S2 system," in *Proc. Int. Conf. Wireless Commun. Signal Process. (WCSP)*, Oct. 2010, pp. 1–5.
[46] N. C. Beaulieu, C. C. Tan, and M. O. Damen, "A 'better than' Nyquist pulse," *IEEE Commun. Lett.*, vol. 5, no. 9, pp. 367–368, Sep. 2001.
[47] U. Mengali and A. N. D'Andrea, *Synchronization Techniques for Digital Receivers*. New York, NY, USA: Plenum, 1997.
[48] H. Minn, M. Zeng, and V. K. Bhargava, "On timing offset estimation for OFDM systems," *IEEE Commun. Lett.*, vol. 4, no. 7, pp. 242–244, Jul. 2000.
[49] N. Souto, R. Dinis, and J. C. Silva, "Impact of channel estimation errors on SC-FDE systems," *IEEE Trans. Commun.*, vol. 62, no. 5, pp. 1530–1540, May 2014.
[50] P. Singh, H. B. Mishra, A. K. Jagannatham, and K. Vasudevan, "Semi-blind, training, and data-aided channel estimation schemes for MIMO-FBMC-OQAM systems," *IEEE Trans. Signal Process.*, vol. 67, no. 18, pp. 4668–4682, Sep. 2019.

XI PAN received the B.S., M.S., and Ph.D. degrees from the Beijing Institute of Technology, Beijing, China, in 1999, 2002, and 2007, respectively. From 2011 to 2012, she was a Visiting Scholar with the College of Engineering and Computer Science, The Australian National University. She is currently an Associate Professor with the School of Mechatronical Engineering, Beijing Institute of Technology. She has been working on a range of research projects, including four projects of NSFC, three Defence Key Laboratory funds, two Advance Research Programs. She holds more than ten patents. Her research interests include target tracking and ranging technique and short range radar signal processing.

CHAOXING YAN (Member, IEEE) received the Ph.D. degree in communication and information system from the Beijing Institute of Technology, China, in 2012. Since March 2012, he has been with the Beijing Research Institute of Telemetry, where he is currently a Senior Engineer. From July 2017 to December 2017, he was a Visiting Scholar with the Next-Generation Wireless Group chaired by Prof. Lajos Hanzo, School of Electronics and Computer Science, University of Southampton, U.K. He is also selected into the Youth Outstanding Talent Support Program (2019) of China Aerospace Science and Technology Corporation (CASC). He is the author of several scientific papers and holds over 40 patents. His primary research interests include wireless communication and networking techniques in terrestrial networks, UAV networks, satellite, and space communication networks. He serves as the Session Chair for IEEE/CIC ICCC 2018 and a reviewer for several IEEE journals.

JIANKANG ZHANG (Senior Member, IEEE) received the B.Sc. degree in mathematics and applied mathematics from the Beijing University of Posts and Telecommunications, in 2006, and the Ph.D. degree in communication and information systems from Zhengzhou University, in 2012. He is currently a Senior Lecturer with Bournemouth University. Prior to joining in Bournemouth University, he was a Senior Research Fellow with the University of Southampton, U.K. From 2009 to 2011, he was a Visiting Ph.D. Student with the School of Electronics and Computer Science, University of Southampton. From 2012 to 2013, he was a Lecturer with Zhengzhou University, where he was an Associate Professor, from 2013 to 2014. From 2013 to 2014, he was a Postdoctoral Researcher with McGill University, Canada. His research interests include aeronautical communications, aeronautical networks, and evolutionary algorithms. He was a recipient of a number of academic awards, including the Excellent Doctoral Dissertation of Henan Province, China; the Youth Science and Technology Award of Henan Province, China; and the Innovative Talent of Colleges and Universities of Henan Province, China. He also serves as an Associate Editor for IEEE Access.